Chemical Science

ROYAL SOCIETY OF CHEMISTRY

EDGE ARTICLE

View Article Online
View Journal | View Issue

Cite this: *Chem. Sci.*, 2020, **11**, 4410

All publication charges for this article have been paid for by the Royal Society of Chemistry

Tetrazine as a general phototrigger to turn on fluorophores†

Axel Loredo, ‡[a] Juan Tang,‡[a] Lushun Wang,‡[a] Kuan-Lin Wu,[a] Zane Peng[b] and Han Xiao *[abc]

Light-activated fluorescence affords a powerful tool for monitoring subcellular structures and dynamics with enhanced temporal and spatial control of the fluorescence signal. Here, we demonstrate a general and straightforward strategy for using a tetrazine phototrigger to design photoactivatable fluorophores that emit across the visible spectrum. Tetrazine is known to efficiently quench the fluorescence of various fluorophores *via* a mechanism referred to as through-bond energy transfer. Upon light irradiation, restricted tetrazine moieties undergo a photolysis reaction that generates two nitriles and molecular nitrogen, thus restoring the fluorescence of fluorophores. Significantly, we find that this strategy can be successfully translated and generalized to a wide range of fluorophore scaffolds. Based on these results, we have used this mechanism to design photoactivatable fluorophores targeting cellular organelles and proteins. Compared to widely used phototriggers (*e.g.*, *o*-nitrobenzyl and nitrophenethyl groups), this study affords a new photoactivation mechanism, in which the quencher is photodecomposed to restore the fluorescence upon light irradiation. Because of the exclusive use of tetrazine as a photoquencher in the design of fluorogenic probes, we anticipate that our current study will significantly facilitate the development of novel photoactivatable fluorophores.

Received 19th February 2020
Accepted 2nd April 2020

DOI: 10.1039/d0sc01009j

rsc.li/chemical-science

Introduction

Photoactivatable fluorophores, also called turn-on fluorophores,[1–7] have numerous advanced biological applications, including detection and release of ions[8–11] and metabolites,[12–15] monitoring of enzyme activity,[16–19] and multiple types of specialized microscopy.[7,20–25] Most of these photoactivatable fluorophores are masked by a reactive "cage" group intimately attached to the fluorophore to alter its photophysical properties or to serve as an energy-transfer agent for use in a fluorescence resonance energy transfer (FRET) pair.[26] Upon light or chemical treatment, these "caged" fluorophores undergo chemical reactions that release the "cage" groups to regenerate the fluorophores in their active forms.[27–35] The timing and site of fluorescence restoration are therefore controlled by the application of the "de-caging" treatment. For two reasons, tetrazine has recently emerged as a very effective quenching group in the design of fluorogenic fluorophores. First, tetrazine absorbs visible light at around 500–550 nm, making it an ideal quencher for a series of fluorophores that are useful for FRET studies.[36–39] Second, tetrazine derivatives can undergo an Inverse Electron Demand Diels–Alder (IEDDA) cycloaddition reaction with strained hydrophobic alkenes, such as *trans*-cyclooctene,[40] cyclopropenes,[41] or norbornene.[42] These bioorthogonal reactions are characterized by fast reaction rates and high selectivity. By taking advantage of this dual functionality, tetrazine has been conjugated *via* a flexible linker to rhodamine,[39] boron dipyrromethene (BODIPY) and Oregon Green[37] and then used as a quencher moiety through the FRET mechanism. Upon destruction of the tetrazine core with strained alkenes in the IEDDA reaction, fluorescence enhancement up to 20-fold has been observed for these fluorophores.[37]

To further improve the quenching efficiency, recent studies have used tetrazine to quench fluorophore fluorescence *via* through-bond energy transfer (TBET),[43–49] a mechanism that does not require spectral overlap between donors and acceptors.[50] In this context, tetrazine was conjugated to fluorophore donors using a conjugated linker that allows for faster energy transfer through bonds relative to nonradiative decay processes. The resulting "caged" fluorophores exhibited superb fluorescence turn-on upon reaction with *trans*-cyclooctene,[45] allowing for enhanced imaging of cellular components due to reduced background fluorescence.

[a]*Department of Chemistry, Rice University, 6100 Main Street, Houston, Texas, 77005, USA. E-mail: han.xiao@rice.edu*

[b]*Department of Biosciences, Rice University, 6100 Main Street, Houston, Texas, 77005, USA*

[c]*Department of Bioengineering, Rice University, 6100 Main Street, Houston, Texas, 77005, USA*

† Electronic supplementary information (ESI) available. See DOI: 10.1039/d0sc01009j

‡ These authors contributed equally.

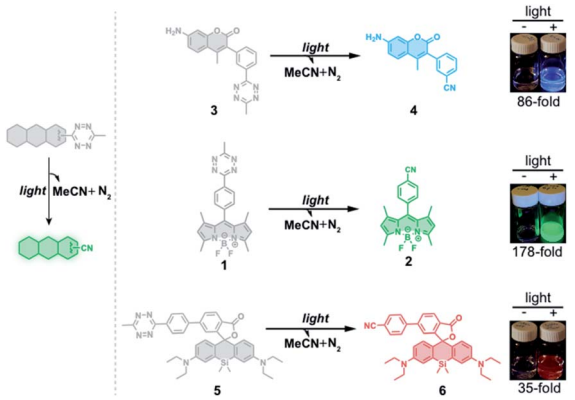

Fig. 1 Schematic representation of fluorescence turn-on of tetrazine-fluorophore derivatives using the tetrazine phototrigger.

Despite the potential for broad applications of tetrazine-based fluorogenic fluorophores, large and strained hydrophobic alkenes have been exclusively used as chemical triggers for restoring fluorescence. Compared to decaging using chemical triggers, photo-decaging offers superior spatial and temporal control and is generally considered to be more biocompatible. Tetrazine can undergo photolysis, generating relatively inert, unobtrusive nitriles and molecular nitrogen.[51] Gaseous tetrazine is known to absorb visible light that permits the n → π* transition and decomposition with almost unit quantum yield.[52] Taking advantage of this photolysis reaction, tetrazine has been used for studies on protein folding by incorporating it into peptides as a phototrigger to modulate peptide stapling/unstapling after illumination with 330–400 nm light.[53–57] Here, we describe a new approach for conjugating the tetrazine moiety to fluorophores as a phototrigger for initiating fluorophore photoactivation (Fig. 1).

Results and discussion

Photoactivation of BODIPY fluorophores using the tetrazine phototrigger

To test whether the tetrazine motif can be incorporated into fluorophores to generate photoactivatable fluorophores, we synthesized the methyl-*s*-tetrazine-BODIPY conjugate (Tz-BODIPY, **1**, Fig. 1) as described previously.[43] The fluorescence quantum yield for **1** ($\Phi < 0.01$) in acetonitrile is much lower than that for the nitrile counterpart **2** ($\Phi = 0.60$) (Table 1), suggesting the possibility that the photolysis of tetrazine could be used to induce fluorogenic activation of Tz-BODIPY. Indeed, following 20 minute irradiation with 254 nm light (1400 μW cm^{-2}), the fluorescence intensity of Tz-BODIPY increased dramatically. The observed 178-fold fluorescence enhancement at 509 nm is similar to the 340-fold fluorescence increase reported in the literature after chemical triggering with *trans*-cyclooctene (Fig. 2).[43]

The photolysis product was further analyzed by ^{1}H NMR and ESI-MS analysis. Upon light irradiation, the aromatic protons of Tz-BODIPY exhibited an upfield shift. Signals corresponding to phenyl and methyl protons at 8.68, 7.65, 6.12, 3.04, 2.51 and 1.47 ppm gradually disappeared, and new signals appeared at 7.88, 7.56, 6.11, 2.49 and 1.37 ppm (Fig. 2A). These new signals were identical to those observed with synthesized *p*-cyanophenyl-BODIPY (CN-BODIPY, **2**, Fig. 2). ESI-MS analysis of the reaction product yielded an observed mass of 350.16, in agreement with the calculated mass of CN-BODIPY ([M + H$^+$] = 350.15, Fig. S1†). These data, therefore, demonstrate that the photolysis product of Tz-BODIPY is its nitrile counterpart, CN-BODIPY.

Design of photoactivatable fluorophores using the tetrazine phototrigger

To demonstrate that the tetrazine motif can be used as a general phototrigger, methyl-*s*-tetrazine-coumarin (Tz-Coumarin, **3**) and methyl-*s*-tetrazine-silicon rhodamine (Tz-Si-Rhodamine, **5**) were prepared (Fig. 1).[45,47] Next, we characterized the spectroscopic and photochemical properties of these fluorophores with the tetrazine phototrigger and their photolysis products using UV-vis and fluorescence spectroscopies (Table 1 and Fig. S2†). As shown in Table 1, the introduction of the tetrazine phototrigger in all the tested fluorophores led to significant reductions in quantum yield. To assess the efficiency of photoactivation for the tetrazine phototrigger, UV-vis and

Table 1 Photophysical data of tetrazine-caged fluorophores and their nitrile derivatives

Compound number	Compound	λ_{abs} (nm)	λ_{em} (nm)	$\varepsilon \times 10^4$ (M^{-1} cm^{-1})	Φ_{MeCN}	Fluorescence increase[d]
1	Tz-BODIPY	490	509	1.9	0.004[a]	178-Fold
2	CN-BODIPY	492	509	3.6	0.60[a]	—
3	Tz-Coumarin	347	416	1.8	<0.001[b]	86-Fold
4	CN-Coumarin	351	417	1.9	0.19[b]	—
5	Tz-Si-Rhodamine	651	671	2.6	0.011[c]	35-Fold
6	CN-Si-Rhodamine[e]	652	671	2.4	0.34[c]	—
7	Tz-BODIPY-MOR	495	511	2.6	0.03[a]	45-Fold
8	Tz-BODIPY-Ts	492	510	1.8	0.02[a]	36-Fold
9	Tz-BODIPY-TPP	494	509	3.0	0.007[a]	97-Fold
10	Tz-BODIPY-Halo	491	509	2.4	0.002[a]	141-Fold

[a] Fluorescein in 0.1 M NaOH. [b] Quinine sulfate in 0.5 M H_2SO_4 was used as a reference for measuring the quantum yields. [c] Rhodamine B in water was used as a reference for measuring the quantum yields. [d] 254 nm light activation (1400 μW cm^{-2}). [e] Measured after irradiation of compound **5** with 254 nm light.

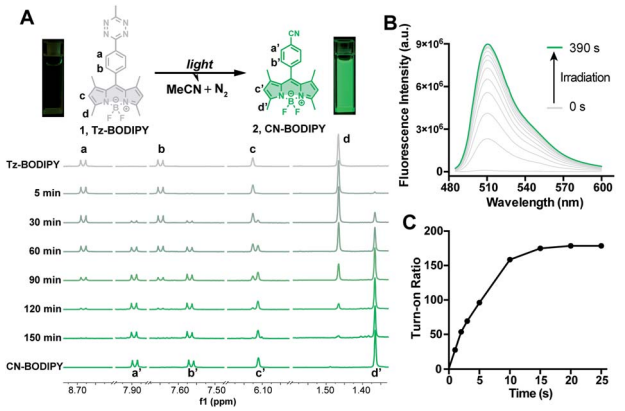

Fig. 2 (A) Reaction scheme of light photolysis of Tz-BODIPY **1** and the ^{1}H NMR spectra of Tz-BODIPY **1** obtained at the indicated light irradiation times using a 254 nm handheld UV light. (B) Fluorescent emission spectral change of Tz-BODIPY **1** after light activation. (C) Change of fluorescence intensity at 509 nm during light irradiation using a 254 nm handheld UV light.

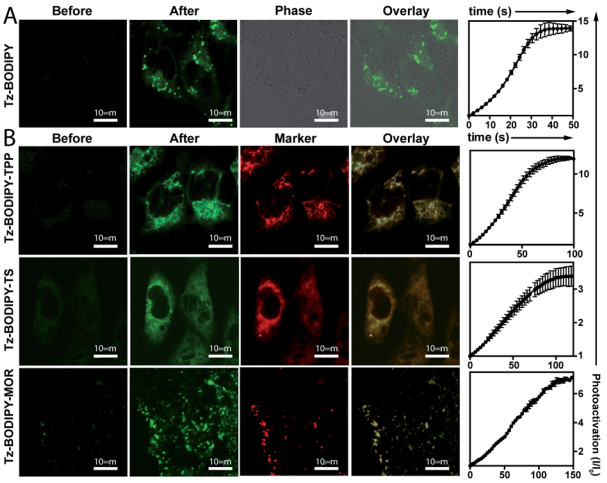

Fig. 3 (A) Photoactivation of Tz-BODIPY derivatives in A431 cells using 405 nm laser activation. Confocal images were obtained before and after 405 nm light activation of Tz-BODIPY derivatives. Scale bar = 10 μm. (B) Photoactivation of organelle-targeting Tz-BODIPY probes in A431 cells. A431 cells were incubated with Tz-BODIPY-TPP **9**, Tz-BODIPY-MOR **7**, or Tz-BODIPY-Ts **8**, and the corresponding commercial organelle-targeting dye, followed by photoactivation using a 405 nm laser. Commercial MitoView™ 633, ER-Tracker™ Blue-White DPX, and LysoView™ 633 were used as markers for mitochondria, endoplasmic reticulum, and lysosomes, respectively. Scale bar = 10 μm.

fluorescence spectra were recorded after different irradiation times (Fig. S3†). To our delight, the fluorescence intensity of the Tz-Coumarin and Tz-Si-Rhodamine molecules increased by 86 and 35-fold, respectively, suggesting that the introduction of a tetrazine phototrigger could be a general strategy for preparing photoactivatable fluorophores with diverse structures.

Fluorescence imaging using Tz-BODIPY derivatives

Having established the excellent photoactivation properties of the tetrazine phototrigger, we sought to explore the utility of the tetrazine phototrigger for biological imaging. Because of its exceptional turn-on properties, we have used the Tz-BODIPY derivatives in the following study. Ultraviolet light has limited applications as a biological initiator, due to its poor tissue penetration and high phototoxicity. To investigate whether light with longer wavelengths can initiate the tetrazine photolysis reaction, we irradiated Tz-BODIPY with light at 254 nm, 365 nm, and 405 nm, respectively. Gratifyingly, significant fluorescence enhancement was observed upon irradiation at 405 nm, a wavelength that is commonly available in commercial microscopes (Fig. S4†). This wavelength was therefore used for activation in the biological imaging study described below. For this study, it was also important to examine the cellular uptake and intracellular photoactivation of Tz-BODIPY derivatives. A431 cells were incubated with Tz-BODIPY, and intracellular photoactivation was monitored by confocal laser scanning microscopy. As shown in Fig. 3A, while negligible fluorescence was observed before photoactivation of Tz-BODIPY, a 14-fold increase in intracellular green fluorescence was observed after irradiation with 405 nm laser light, suggesting not only good photoactivation but also good cell permeability of Tz-BODIPY. However, Tz-Coumarin and Tz-Si-Rhodamine did not exhibit high fluorescence turn-on in A431 cells due to the high autofluorescence and the possible background fluorescence from the open spiroester form before the irradiation process (Fig. S5†).

Synthesis of organelle-targeting Tz-BODIPYs and their applications in fluorescence imaging

The combination of subcellular targeting and photodecaging has provided a platform for precise control of site-specific molecular release.[58–61] Accordingly, we explored the possibility of combining a tetrazine phototrigger with subcellular targeting moieties. To stably conjugate organelle-targeting moieties to Tz-BODIPY without affecting the its photochemical properties, we developed a robust synthetic approach for functionalizing the BODIPY molecule (Fig. 4).

In brief, an aldehyde moiety was first introduced at position 2 of BODIPY using the Vilsmeier–Haack reaction,[62] followed by a Pinnick oxidation to yield carboxylic acid.[63] The resulting carboxyl-functionalized BODIPY was obtained in good yield and coupled to amine-bearing organelle-targeting groups using *N*-[(dimethylamino)-1*H*-1,2,3-triazo[4,5-*b*]pyridin-1-ylmethylene]-*N*-methylmethanaminium hexafluorophosphate-*N*-oxide (HATU)-mediated amide coupling to yield organelle-targeting Tz-BODIPYs. Using this protocol, we have prepared Tz-BODIPY with the following organelle-directing groups: phenyl sulfonamide (Tz-BODIPY-Ts, endoplasmic reticulum targeting, Fig. 4),[64] morpholine (Tz-BODIPY-MOR, lysosome targeting, Fig. 4),[65] and triphenylphosphonium (Tz-BODIPY-TPP, mitochondria targeting, Fig. 4).[66] To our delight, all three organelle-targeting Tz-BODIPYs were stable in the absence of light (Fig. S6†) and exhibited significant fluorescence enhancement

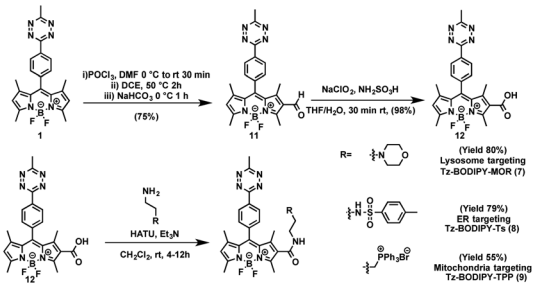

Fig. 4 Synthetic route to organelle-targeting Tz-BODIPYs.

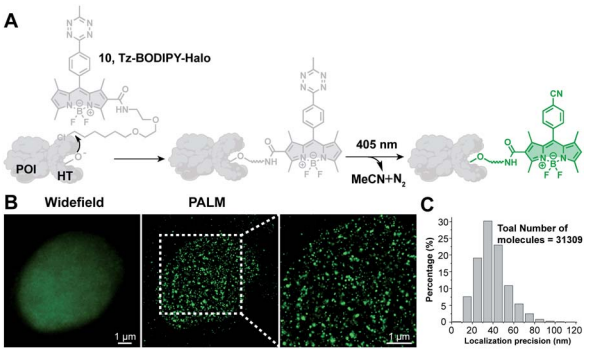

Fig. 5 PALM imaging of histone proteins using the Tz-BODIPY-Halo probe. (A) Site-specific labeling of the protein of interest (POI) with the Tz-BODIPY-Halo probe for fluorescence imaging. (B) Widefield image and corresponding PALM images of H2B labeled with H2B-HaloTag in CHO–K1 cells. (C) Histogram plot of the localization accuracy of PALM images in (B). Scale bar = 1 μm.

after light irradiation in acetonitrile (Table 1, Fig. S7†). In order to evaluate the localization of these organelle-targeting Tz-BODIPY derivatives, confocal laser scanning microscopy was carried out on A431 cells. Commercial MitoView™ 633, ER-Tracker™ Blue-White DPX, and LysoView™ 633 were used as markers for mitochondria, endoplasmic reticulum, and lysosomes, respectively. All three BODIPY compounds had negligible fluorescence prior to irradiation with the 405 nm laser, but exhibited distinct increases in fluorescence signals following tetrazine triggering. Turn-on ratios of 12, 3.5 and 7 were observed for Tz-BODIPY-TPP **9**, Tz-BODIPY-MOR **7**, and Tz-BODIPY-Ts **8**, respectively (Fig. 3B).

Most importantly, good co-localization was observed between the green fluorescence of the BODIPY compounds and the red fluorescence of the corresponding organelle-targeting commercial dyes (Fig. 3B). This is reflected by the high Pearson's correlation coefficients found for Tz-BODIPY-Ts (γ = 0.85), Tz-BODIPY-MOR (γ = 0.84), and Tz-BODIPY-TPP (γ = 0.75). These data demonstrate that the photoactivability of Tz-BODIPYs can be productively combined with the specificity of subcellular targeting molecules for organelle imaging.

Super-resolution imaging using tetrazine-caged BODIPY fluorophores

Photoactivatable fluorescent probes should find useful applications in super-resolution imaging (*e.g.*, Photoactivated Localization Microscopy, PALM; Stochastic Optical Reconstruction Microscopy, STORM),[67,68] a technology that allows imaging beyond the diffraction limit.[21,22,69–72] Thus, we explored the possibility of using Tz-BODIPY for PALM imaging. To site-specifically label proteins of interest, we used HaloTag labeling technology,[73–75] which is based on covalent bond formation between HaloTag-fused proteins and a synthetic HaloTag ligand. The HaloTag tetrazine-BODIPY conjugate (Fig. 5A) was synthesized following a strategy similar to that used for the organelle-targeting probes. The fluorescence quantum yield of the compound (Φ = 0.002, Table 1) was in the range of that of the other synthesized Tz-BODIPY dyes. After 40 minutes of 254 nm light irradiation using a handheld UV lamp, a 141-fold fluorescence enhancement was observed (Table 1 and Fig. S7†), while no significant fluorescence increase was detected in the absence of light (Fig. S8†). Next, CHO-K1 cells expressing histone 2B (H2B)-HaloTag were incubated with Tz-BODIPY-Halo **10** for 30 min and then incubated in fresh culture medium for another 30 min. Intracellular photoactivation was initially monitored *via* confocal laser scanning microscopy. As shown in Fig. S9,† an 8-fold increase in intracellular fluorescence was observed after 405 nm laser irradiation. Co-incubation of compound **10** with the commercial nuclear dye, DRAQ5, confirmed a distinct nuclear localization pattern for the histone conjugate. Subsequently, we utilized Tz-BODIPY-Halo **10** for PALM imaging of histone-2B in CHO-K1 cells by activating Tz-BODIPY-Halo with the 405 nm laser contained in the microscope (Fig. S9†). By capturing sets of 20 000–30 000 imaging frames, we reconstructed the super-resolution image of H2B localization (Fig. 5B). Compared to conventional widefield fluorescence imaging, the reconstructed PALM imaging exhibits much better resolution along with high molecular accuracy (*ca.* 40.8 nm) (Fig. 5C). It is worth mentioning that this PALM imaging can be performed under physiological conditions without the need for cytotoxic reducing buffers to induce the fluorescence on–off transition cycles. Taken together, our data demonstrate that the tetrazine-caged BODIPY fluorophores developed in this study are compatible with existing protein labeling technologies and can be used for super-resolution imaging of living cells.

Conclusions

In summary, we have designed and characterized a unique class of photoactivatable tetrazine-based probes in which the tetrazine moiety serves as both a fluorescence quencher and a phototrigger. The utility of these turn-on probes is further demonstrated by our success with organelle imaging and super-resolution imaging under physiological conditions that do not require the use of a cytotoxic imaging cocktail. We are currently exploring the use of a longer wavelength two-photon laser to dissociate the tetrazine moiety, as this process has been reported for tetrazine by measuring the evolution of HCN after irradiation at 492 and 532 nm.[76,77]

In contrast to the widely used phototriggers (*e.g.*, *o*-nitrobenzyl and nitrophenethyl groups) altering the electron

structure of fluorescent molecules upon light irradiation,[78–80] this study affords a new photoactivation mechanism, in which the TBET quencher is photodecomposed to restore the fluorescence. Besides serving as a TBET quencher, the tetrazine moiety has also been exclusively used as a FRET acceptor to design FRET-based fluorogenic probes. Thus, we believe that this work will open up the possibility of using tetrazine as a photo-trigger to activate other FRET-based fluorogenic probes.

Conflicts of interest

There are no conflicts to declare.

Acknowledgements

This work was supported by the Cancer Prevention and Research Institute of Texas (CPRIT, RR170014), the Robert A. Welch Foundation (C-1970), the Hamill Innovation Award (Hamill Foundation), the John S. Dunn Foundation Collaborative Research Award (Gulf Coast Consortia) and the NIH (R35-GM133706). H. X. is a Cancer Prevention & Research Institute of Texas (CPRIT) Scholar in Cancer Research.

Notes and references

1 G. A. Krafft, W. R. Sutton and R. T. Cummings, *J. Am. Chem. Soc.*, 1988, **110**, 301–303.
2 Y. Zhao, Q. Zheng, K. Dakin, K. Xu, M. L. Martinez and W.-H. Li, *J. Am. Chem. Soc.*, 2004, **126**, 4653–4663.
3 T. Kobayashi, Y. Urano, M. Kamiya, T. Ueno, H. Kojima and T. Nagano, *J. Am. Chem. Soc.*, 2007, **129**, 6696–6697.
4 J. Fölling, V. Belov, R. Kunetsky, R. Medda, A. Schönle, A. Egner, C. Eggeling, M. Bossi and S. W. Hell, *Angew. Chem., Int. Ed.*, 2007, **46**, 6266–6270.
5 G. T. Dempsey, M. Bates, W. E. Kowtoniuk, D. R. Liu, R. Y. Tsien and X. Zhuang, *J. Am. Chem. Soc.*, 2009, **131**, 18192–18193.
6 J. C. Vaughan, G. T. Dempsey, E. Sun and X. Zhuang, *J. Am. Chem. Soc.*, 2013, **135**, 1197–1200.
7 J. Tang, M. A. Robichaux, K.-L. Wu, J. Pei, N. T. Nguyen, Y. Zhou, T. G. Wensel and H. Xiao, *J. Am. Chem. Soc.*, 2019, **141**, 14699–14706.
8 P. Du and S. J. Lippard, *Inorg. Chem.*, 2010, **49**, 10753–10755.
9 C.-H. Lee, H.-J. Yoon, J.-S. Shim and W.-D. Jang, *Chem.–Eur. J.*, 2012, **18**, 4513–4516.
10 H. K. Agarwal, R. Janicek, S.-H. Chi, J. W. Perry, E. Niggli and G. C. R. Ellis-Davies, *J. Am. Chem. Soc.*, 2016, **138**, 3687–3693.
11 C. Deo, S.-H. Sheu, J. Seo, D. E. Clapham and L. D. Lavis, *J. Am. Chem. Soc.*, 2019, **141**, 13734–13738.
12 S. Resa, A. Orte, D. Miguel, J. M. Paredes, V. Puente-Muñoz, R. Salto, M. D. Giron, M. J. Ruedas-Rama, J. M. Cuerva, J. M. Alvarez-Pez and L. Crovetto, *Chem.–Eur. J.*, 2015, **21**, 14772–14779.
13 Y. Yue, F. Huo, P. Ning, Y. Zhang, J. Chao, X. Meng and C. Yin, *J. Am. Chem. Soc.*, 2017, **139**, 3181–3185.
14 R. R. Nani, A. P. Gorka, T. Nagaya, H. Kobayashi and M. J. Schnermann, *Angew. Chem., Int. Ed.*, 2015, **54**, 13635–13638.
15 R. R. Nani, A. P. Gorka, T. Nagaya, T. Yamamoto, J. Ivanic, H. Kobayashi and M. J. Schnermann, *ACS Cent. Sci.*, 2017, **3**, 329–337.
16 H. Li, Q. Yao, F. Xu, N. Xu, R. Duan, S. Long, J. Fan, J. Du, J. Wang and X. Peng, *Biomaterials*, 2018, **179**, 1–14.
17 Y. Takaoka, H. Tsutsumi, N. Kasagi, E. Nakata and I. Hamachi, *J. Am. Chem. Soc.*, 2006, **128**, 3273–3280.
18 H. Ai, K. L. Hazelwood, M. W. Davidson and R. E. Campbell, *Nat. Methods*, 2008, **5**, 401–403.
19 D. Cheng, Y. Pan, L. Wang, Z. Zeng, L. Yuan, X. Zhang and Y.-T. Chang, *J. Am. Chem. Soc.*, 2017, **139**, 285–292.
20 L. D. Lavis, T.-Y. Chao and R. T. Raines, *ACS Chem. Biol.*, 2006, **1**, 252–260.
21 M. Bates, B. Huang, G. T. Dempsey and X. Zhuang, *Science*, 2007, **317**, 1749–1753.
22 S.-H. Shim, C. Xia, G. Zhong, H. P. Babcock, J. C. Vaughan, B. Huang, X. Wang, C. Xu, G.-Q. Bi and X. Zhuang, *Proc. Natl. Acad. Sci.*, 2012, **109**, 13978–13983.
23 J. B. Grimm, B. P. English, H. Choi, A. K. Muthusamy, B. P. Mehl, P. Dong, T. A. Brown, J. Lippincott-Schwartz, Z. Liu, T. Lionnet and L. D. Lavis, *Nat. Methods*, 2016, **13**, 985–988.
24 C. S. Wijesooriya, J. A. Peterson, P. Shrestha, E. J. Gehrmann, A. H. Winter and E. A. Smith, *Angew. Chem., Int. Ed.*, 2018, **57**, 12685–12689.
25 F. M. Jradi and L. D. Lavis, *ACS Chem. Biol.*, 2019, **14**, 1077–1090.
26 L. Yuan, W. Lin, K. Zheng and S. Zhu, *Acc. Chem. Res.*, 2013, **46**, 1462–1473.
27 G. Zheng, Y.-M. Guo and W.-H. Li, *J. Am. Chem. Soc.*, 2007, **129**, 10616–10617.
28 V. N. Belov, C. A. Wurm, V. P. Boyarskiy, S. Jakobs and S. W. Hell, *Angew. Chem., Int. Ed.*, 2010, **49**, 3520–3523.
29 J. A. Peterson, C. Wijesooriya, E. J. Gehrmann, K. M. Mahoney, P. P. Goswami, T. R. Albright, A. Syed, A. S. Dutton, E. A. Smith and A. H. Winter, *J. Am. Chem. Soc.*, 2018, **140**, 7343–7346.
30 P. P. Goswami, A. Syed, C. L. Beck, T. R. Albright, K. M. Mahoney, R. Unash, E. A. Smith and A. H. Winter, *J. Am. Chem. Soc.*, 2015, **137**, 3783–3786.
31 Y. Zhou, K. Chu, H. Zhen, Y. Fang and C. Yao, *Spectrochim. Acta, Part A*, 2013, **106**, 197–202.
32 Y. Yu, B. Czepukojc, C. Jacob, Y. Jiang, M. Zeller, C. Brückner and J.-L. Zhang, *Org. Biomol. Chem.*, 2013, **11**, 4613–4621.
33 L. Yuan, L. Wang, B. K. Agrawalla, S.-J. Park, H. Zhu, B. Sivaraman, J. Peng, Q.-H. Xu and Y.-T. Chang, *J. Am. Chem. Soc.*, 2015, **137**, 5930–5938.
34 P. Klán, T. Šolomek, C. G. Bochet, A. Blanc, R. Givens, M. Rubina, V. Popik, A. Kostikov and J. Wirz, *Chem. Rev.*, 2013, **113**, 119–191.
35 B. Roubinet, M. Bischoff, S. Nizamov, S. Yan, C. Geisler, S. Stoldt, G. Y. Mitronova, V. N. Belov, M. L. Bossi and S. W. Hell, *J. Org. Chem.*, 2018, **83**, 6466–6476.

36 R. J. Blizzard, D. R. Backus, W. Brown, C. G. Bazewicz, Y. Li and R. A. Mehl, *J. Am. Chem. Soc.*, 2015, **137**, 10044–10047.
37 N. K. Devaraj, S. Hilderbrand, R. Upadhyay, R. Mazitschek and R. Weissleder, *Angew. Chem., Int. Ed.*, 2010, **49**, 2869–2872.
38 K. Lang, L. Davis, J. Torres-Kolbus, C. Chou, A. Deiters and J. W. Chin, *Nat. Chem.*, 2012, **4**, 298–304.
39 B. L. Oliveira, Z. Guo, O. Boutureira, A. Guerreiro, G. Jiménez-Osés and G. J. L. Bernardes, *Angew. Chem., Int. Ed.*, 2016, **55**, 14683–14687.
40 M. L. Blackman, M. Royzen and J. M. Fox, *J. Am. Chem. Soc.*, 2008, **130**, 13518–13519.
41 D. M. Patterson, L. A. Nazarova, B. Xie, D. N. Kamber and J. A. Prescher, *J. Am. Chem. Soc.*, 2012, **134**, 18638–18643.
42 J. Sauer, G. R. Pabst, U. Holland, H.-S. Kim and S. Loebbecke, *Eur. J. Org. Chem.*, 2001, **2001**, 697–706.
43 J. C. T. Carlson, L. G. Meimetis, S. A. Hilderbrand and R. Weissleder, *Angew. Chem., Int. Ed.*, 2013, **52**, 6917–6920.
44 H. Wu, J. Yang, J. Šečkutė and N. K. Devaraj, *Angew. Chem., Int. Ed.*, 2014, **53**, 5805–5809.
45 L. G. Meimetis, J. C. T. Carlson, R. J. Giedt, R. H. Kohler and R. Weissleder, *Angew. Chem., Int. Ed.*, 2014, **53**, 7531–7534.
46 G. Knorr, E. Kozma, A. Herner, E. A. Lemke and P. Kele, *Chem.–Eur. J.*, 2016, **22**, 8972–8979.
47 E. Kozma, G. E. Girona, G. Paci, E. A. Lemke and P. Kele, *Chem. Commun.*, 2017, **53**, 6696–6699.
48 A. Wieczorek, P. Werther, J. Euchner and R. Wombacher, *Chem. Sci.*, 2017, **8**, 1506–1510.
49 Y. Lee, W. Cho, J. Sung, E. Kim and S. B. Park, *J. Am. Chem. Soc.*, 2018, **140**, 974–983.
50 Y.-J. Gong, X.-B. Zhang, C.-C. Zhang, A.-L. Luo, T. Fu, W. Tan, G.-L. Shen and R.-Q. Yu, *Anal. Chem.*, 2012, **84**, 10777–10784.
51 R. M. Hochstrasser and D. S. King, *J. Am. Chem. Soc.*, 1975, **97**, 4760–4762.
52 J. H. Meyling, R. P. Van Der Werf and D. A. Wiersma, *Chem. Phys. Lett.*, 1974, **28**, 364–372.
53 M. J. Tucker, J. R. Courter, J. Chen, O. Atasoylu, A. B. Smith and R. M. Hochstrasser, *Angew. Chem., Int. Ed.*, 2010, **49**, 3612–3616.
54 M. J. Tucker, M. Abdo, J. R. Courter, J. Chen, A. B. Smith and R. M. Hochstrasser, *J. Photochem. Photobiol., A*, 2012, **234**, 156–163.
55 M. Abdo, S. P. Brown, J. R. Courter, M. J. Tucker, R. M. Hochstrasser and A. B. Smith, *Org. Lett.*, 2012, **14**, 3518–3521.
56 J. R. Courter, M. Abdo, S. P. Brown, M. J. Tucker, R. M. Hochstrasser and A. B. Smith, *J. Org. Chem.*, 2014, **79**, 759–768.
57 S. P. Brown and A. B. Smith, *J. Am. Chem. Soc.*, 2015, **137**, 4034–4037.
58 S. Chalmers, S. T. Caldwell, C. Quin, T. A. Prime, A. M. James, A. G. Cairns, M. P. Murphy, J. G. McCarron and R. C. Hartley, *J. Am. Chem. Soc.*, 2012, **134**, 758–761.
59 A. Nadler, D. A. Yushchenko, R. Müller, F. Stein, S. Feng, C. Mulle, M. Carta and C. Schultz, *Nat. Commun.*, 2015, **6**, 1–10.
60 N. Wagner, M. Stephan, D. Höglinger and A. Nadler, *Angew. Chem., Int. Ed.*, 2018, **57**, 13339–13343.
61 D. Kand, L. Pizarro, I. Angel, A. Avni, D. Friedmann-Morvinski and R. Weinstain, *Angew. Chem., Int. Ed.*, 2019, **58**, 4659–4663.
62 S. Zhu, J. Bi, G. Vegesna, J. Zhang, F.-T. Luo, L. Valenzano and H. Liu, *RSC Adv.*, 2013, **3**, 4793–4800.
63 H. Geng, C. M. Hill, S. Zhu, H. Liu, L. Huang and S. Pan, *RSC Adv.*, 2013, **3**, 2306–2312.
64 H. Xiao, P. Li, X. Hu, X. Shi, W. Zhang and B. Tang, *Chem. Sci.*, 2016, **7**, 6153–6159.
65 M. Gao, Q. Hu, G. Feng, B. Z. Tang and B. Liu, *J. Mater. Chem. B*, 2014, **2**, 3438–3442.
66 C. W. T. Leung, Y. Hong, S. Chen, E. Zhao, J. W. Y. Lam and B. Z. Tang, *J. Am. Chem. Soc.*, 2013, **135**, 62–65.
67 S. Adhikari, J. Moscatelli, E. M. Smith, C. Banerjee and E. M. Puchner, *Nat. Commun.*, 2019, **10**, 1–12.
68 G. Beliu, A. J. Kurz, A. C. Kuhlemann, L. Behringer-Pliess, M. Meub, N. Wolf, J. Seibel, Z.-D. Shi, M. Schnermann, J. B. Grimm, L. D. Lavis, S. Doose and M. Sauer, *Commun. Biol.*, 2019, **2**, 1–13.
69 G. Y. Mitronova, S. Polyakova, C. A. Wurm, K. Kolmakov, T. Wolfram, D. N. H. Meineke, V. N. Belov, M. John and S. W. Hell, *Eur. J. Org. Chem.*, 2015, **2015**, 337–349.
70 P. Sengupta, S. B. van Engelenburg and J. Lippincott-Schwartz, *Chem. Rev.*, 2014, **114**, 3189–3202.
71 B. Roubinet, M. Weber, H. Shojaei, M. Bates, M. L. Bossi, V. N. Belov, M. Irie and S. W. Hell, *J. Am. Chem. Soc.*, 2017, **139**, 6611–6620.
72 M. K. Lee, P. Rai, J. Williams, R. J. Twieg and W. E. Moerner, *J. Am. Chem. Soc.*, 2014, **136**, 14003–14006.
73 G. V. Los, L. P. Encell, M. G. McDougall, D. D. Hartzell, N. Karassina, C. Zimprich, M. G. Wood, R. Learish, R. F. Ohana, M. Urh, D. Simpson, J. Mendez, K. Zimmerman, P. Otto, G. Vidugiris, J. Zhu, A. Darzins, D. H. Klaubert, R. F. Bulleit and K. V. Wood, *ACS Chem. Biol.*, 2008, **3**, 373–382.
74 Y. Liu, K. Miao, N. P. Dunham, H. Liu, M. Fares, A. K. Boal, X. Li and X. Zhang, *Biochemistry*, 2017, **56**, 1585–1595.
75 Y. Liu, K. Miao, Y. Li, M. Fares, S. Chen and X. Zhang, *Biochemistry*, 2018, **57**, 4663–4674.
76 D. Coulter, D. Dows, H. Reisler and C. Wittig, *Chem. Phys.*, 1978, **32**, 429–435.
77 J. H. Glownia and S. J. Riley, *Chem. Phys. Lett.*, 1980, **71**, 429–435.
78 W. Li and G. Zheng, *Photochem. Photobiol. Sci.*, 2012, **11**, 460–471.
79 F. M. Raymo, *Phys. Chem. Chem. Phys.*, 2013, **15**, 14840–14850.
80 L. Kowalik and J. K. Chen, *Nat. Chem. Biol.*, 2017, **13**, 587–598.